Non-monolithic fabrication of thin-film microelectrode arrays on PMUT transducers as a bimodal neuroscientific investigation tool

Velea, Andrada I.; Wilson, Joshua; Gollhardt, Astrid; Karuthedath, Cyril B.; Thanniyil, Abhilash S.; Giagka, Vasiliki

DOI
10.1109/EMBC40787.2023.10340770

Publication date
2023

Document Version
Final published version

Published in
Proceeding of the 2023 45th Annual International Conference of the IEEE Engineering in Medicine & Biology Society (EMBC)

2023 45th Annual International Conference of the IEEE Engineering in Medicine & Biology Society (EMBC) | 979-8-3503-2447-1/23/$31.00 ©2023 IEEE | DOI: 10.1109/EMBC40787.2023.10340770

Non-monolithic fabrication of thin-film microelectrode arrays on PMUT transducers as a bimodal neuroscientific investigation tool*

Andrada I. Velea, *Student Member, IEEE*, Joshua Wilson, Astrid Gollhardt, Cyril B. Karuthedath, Abhilash S. Thanniyil, and Vasiliki Giagka, *Senior Member, IEEE*

***Abstract*— Ultrasound (US)-based neuromodulation has recently emerged as a spatially selective yet non-invasive alternative to conventional electrically-based neural interfaces. However, the fundamental mechanisms of US neuromodulation are not yet clarified. Thus, there is a need for in-vitro bimodal investigation tools that allow us to compare the effect of US versus electrically-induced neural activity in the vicinity of the transducing element. To this end, we propose a MicroElectrode-MicroTransducer Array (MEMTA), where a dense array of electrodes is co-fabricated on top of a similarly dense array of US transducers.**

In this paper, we test the proof of concept for such co-fabrication using a non-monolithic approach, where, at its most challenging scenario, desired topologies require electrodes to be formed directly on top of fragile piezoelectric micromachined ultrasound transducer (PMUTs) membranes. On top of the PMUTs, a thin-film microelectrode array was developed utilizing microfabrication processes, including metal sputtering, lithography, etching and soft encapsulation. The samples were analysed through focused ion beam–scanning electron microscopy (FIB-SEM), and the results have shown that damage to the membranes does not occur during any of the process steps. This paper proves that the non-monolithic development of a miniaturised bimodal neuroscientific investigation tool can be achieved, thus, opening up a series of possibilities for further understanding and investigation of the nervous system.

I. Introduction

Bioelectronic medicine aims to develop locally specific and reversible therapies based on modulating the electrical, rather than the chemical component, of neural signalling. Neural interfaces that use electricity as a means of stimulation can already achieve increased precision [1] [2]. However, they tend to become more invasive with the increase in spatial selectivity [3]. Ultrasound (US) has recently emerged as another promising spatially-selective neuromodulation modality [4] [5] [6], which comes with the advantage that it can be applied non-invasively. However, the fundamental mechanisms of US neuromodulation have yet to be fully elucidated. Moreover, having a fair comparison between the effects of US-induced and electrically-induced neuromodulation is currently impossible due to the lack of suitable neuroscientific tools. While the induced activity can be recorded via calcium imaging in an in-vitro setup, a high-resolution tool that allows us to deliver both neuromodulation modalities individually, at the exact location is still needed.

Therefore, this paper aims to showcase the possibility of integrating/co-fabricating a high-density microelectrode array (MEA) on an existing array of micromachined ultrasound transducers (MUTs) in a non-monolithic approach. A microelectrode-microtransducer array (MEMTA) could serve as a bimodal investigation tool to elucidate the fundamental mechanisms involved in neuromodulation and enable further neuroscientific discoveries. To demonstrate the feasibility of this approach, this paper has investigated the fabrication of thin-film metal electrodes directly on the surface of the MUTs, while ensuring that damage to the membranes does not occur during the process. A schematic representation of the proposed concept is shown in **figure 1**.

II. Methods

A. Ultrasound transducer array

Arrays of miniaturised US transducers can be developed by dicing films of piezoelectric material (usually PZT) [7]. Alternatively, micromachining techniques can be used to create capacitive or piezoelectric ultrasound transducers (CMUTs and PMUTs, respectively). In this case, a thin membrane suspended above a vacuum cavity vibrates in a flexural mode to produce or receive acoustic waves [8], while a pair of top and bottom electrodes is responsible for the transduction between the electric and acoustic domain. The latter technique lends itself to easier and scalable fabrication

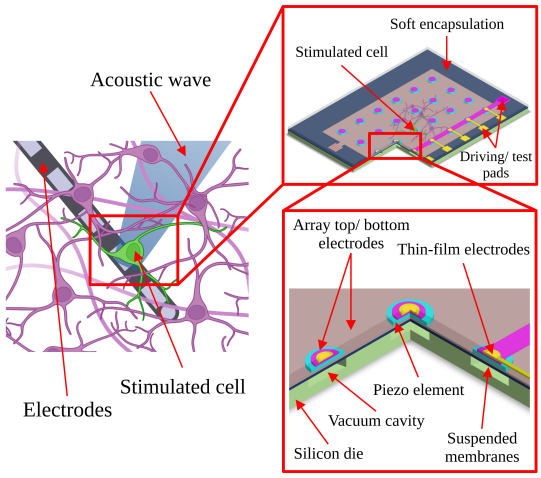

Figure 1. Illustration of the proposed microfabricated bimodal neuroscientific tool.

* Research supported by the Moore4Medical project funded by the ECSEL Joint Undertaking under grant number H2020-ECSEL-2019-IA-876190.

A.I. Velea and V. Giagka are with the Bioelectronics Section, Dept. of Microelectronics, Faculty of Electrical Engineering, Mathematics and Computer Science, Delft University of Technology, the Netherlands (Corresponding author e-mail: A.Velea-1@tudelft.nl).

A.I. Velea, J. Wilson, A. Gollhardt and V. Giagka are with the Fraunhofer Institute for Reliability and Microintegration IZM.

C. Karuthedath and A. S. Thanniyil are with the VTT Technical Research Centre of Finland Ltd.

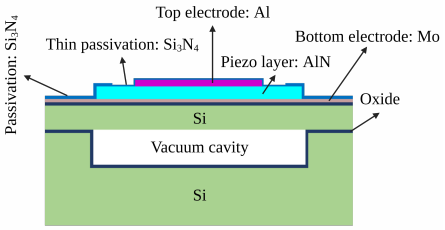

Figure 2. Schematic representation of one PMUT cell of the array used for the investigations. The vibrating membrane comprising top Al and bottom Mo electrodes as well as the piezoelectric material (AlN) are suspended above the vacuum cavity developed within the Si die.

of miniaturised transducers and is fully compatible with microfabrication processes; hence it has been the choice for the transducers presented in this work. Specifically, 2x2 cm silicon (Si) dies, having a densely packed array of cells (1296 cells with a 120 µm pitch), which could be addressed individually or in smaller clusters, provided by VTT, Technical Research Centre Finland Ltd., have been used for the investigations presented in this paper. The structure and material stack of each PMUT is shown in **figure 2**. The substrate comprises a Si layer with vacuum cavities. On top, a silicon dioxide (SiO_2) passivation layer is present. The vibrating element (i.e., aluminium nitride (AlN) layer) is sandwiched between a bottom molybdenum (Mo) and a top aluminium (Al) electrode. Finally, a silicon nitride (SiN) layer acts as passivation for the entire array.

B. Microelectrode array

The MEAs used in this study (**figure 3**) comprise 28 electrodes placed in the centre of the PMUT array with an opening of 40 µm in diameter and a pitch of 120 µm. Smaller pitches that could lead to a denser MEA are also possible, but demonstrating this was out of the scope for this work. Regarding the materials used, soft polymers (i.e., thermoplastic polyurethane (TPU)) were chosen as a substrate and encapsulation, as well as a stack of thin-film metals (titanium (Ti) and gold (Au)) as conductors. Ti is used here as a seed layer to improve the adhesion between the soft polymer-based substrate and Au. On the other hand, Au, which will later be exposed and in contact with the in-vitro medium, has been chosen due to its known biocompatibility characteristics. Although the metal layers can be directly deposited on the existing passivation [9], we chose to deposit an additional layer of TPU to allow the electrodes and pads to extend beyond the rigid PMUT array, enabling integration of MEMTA into flexible devices, for future applications. Due to their

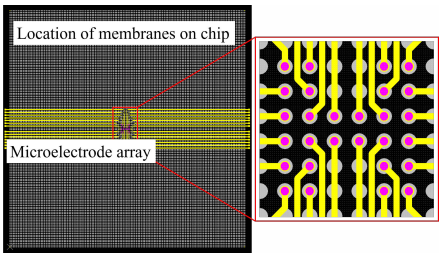

Figure 3. Mask design of the microelectrode array developed on the surface of the PMUTs. In grey, the location of the membranes on the PMUT array. In yellow, the metal layer and in pink, the exposed electrodes.

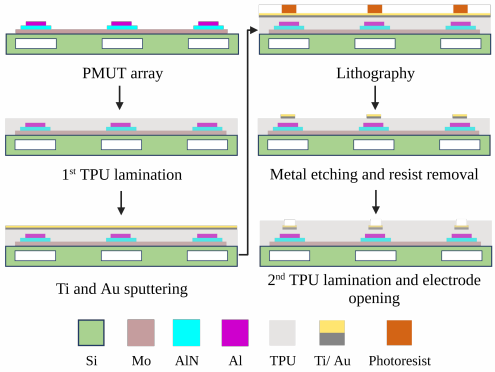

Figure 4. Schematic representation of the fabrication process.

thermoplastic nature, the TPU sheets (Platilon 4201AU, Covestro AG, Germany) will melt and reshape under elevated temperatures, thus ensuring that no interface is present between two individual layers [10] [11].

C. Fabrication of test structures

A schematic representation of the microfabrication process flow used in this work is shown in **figure 4**. First, a 25 µm thick layer of TPU was laminated on top of the PMUT array, using a vacuum applicator (VA 7124-HP7 from Dynachem Automatic Lamination Technologies, Italy) at 160 °C and 6 bar. Next, 50 nm Ti and 50 nm Au were sputtered (500 W power for Ti and 250 W power for Au at $5x10^{-3}$ mbar) on top. Before sputtering, an argon-based (Ar) RF surface pre-treatment was performed for 5 minutes using 50 W of power to further increase the adhesion between the sputtered layer and TPU. Furthermore, an Ar-based surface post-treatment using the same parameters as for the pre-treatment was employed to improve the adhesion between the sputtered layer and the photoresist used during the lithography step. The lithography process uses a 10 µm thick dry negative photoresist film (RY5110, Resonac, Japan) as a mask, laminated at 67 °C and 6 bar, exposed using a micromirror digital imaging system (MDI) (Schmoll Maschinen GmbH, Germany) and developed in sodium carbonate (Na_2CO_3) in a 0.9% concentration. Later, the sputtered metal layer was wet-etched, manually, in a beaker, in a two-step process, using gold stripper 645 from Schloetter for Au, at room temperature and 95% Meltex LTF E53 mixed with 5% hydrogen peroxide (H_2O_2) with a concentration of 30% at 50 °C for Ti. After the removal of the photoresist mask using a mixture of 2-aminoethanol (C_2H_7NO) and potassium hydroxide (KOH) with a concentration of 10-12% at 50 °C, a second TPU layer was laminated at 160 °C and 6 bar.

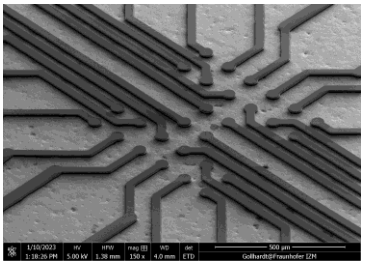

Figure 5. Sample after lithography. The dark grey layer represents the patterned photoresist on top of the metal layer.

Finally, the electrode contacts were exposed by dry etching of the TPU layer using a March PCB 800 system (from Nordson Electronics Solutions, USA). To this end, a second lithography step was required to define the areas to be etched. Instead of a metal hard mask, a thicker photoresist layer (25 µm thick dry resist film RD1225, Resonac, Japan) was laminated at 85 °C and 6 bar. The TPU dry etching process parameters were as follows: 60 °C temperature, 240 mTorr pressure and 4 kW power, using a mixture of several gases: 80% oxygen (O_2), 10% carbon tetrafluoride (CF_4) and 10% Ar, for 2 hours.

D. Analysis methods

After each process step, focused ion beam – scanning electron microscopy (FIB-SEM) was employed to analyse the samples and identify potential failures during fabrication. All FIB cuts were made at locations where membranes only or membranes and electrodes were present.

III. Results and Discussion

For the proposed device, the focus was on developing a MEA on top of an existent PMUT array. To this end, an array of 28 Ti/Au electrodes was designed and fabricated on a TPU layer previously laminated on the PMUT array. **Figure 5** shows the microelectrode array after completion of the lithography steps. To preserve the functionality of the final device, it is crucial to ensure the integrity of each structure but more importantly, of the membrane, after each microfabrication process step. **Figure 6a** illustrates the structure and layer stack of a bare PMUT array as received from the manufacturer. This die was used as a reference during the investigations. **Figure 6b** shows the device after the first fabrication step (i.e., TPU lamination). It can be seen that the structure of the membranes does not present any defects, although the arrays were subjected to elevated temperature (160 °C) and pressure during this step. Important to note are the particles within the TPU layer.

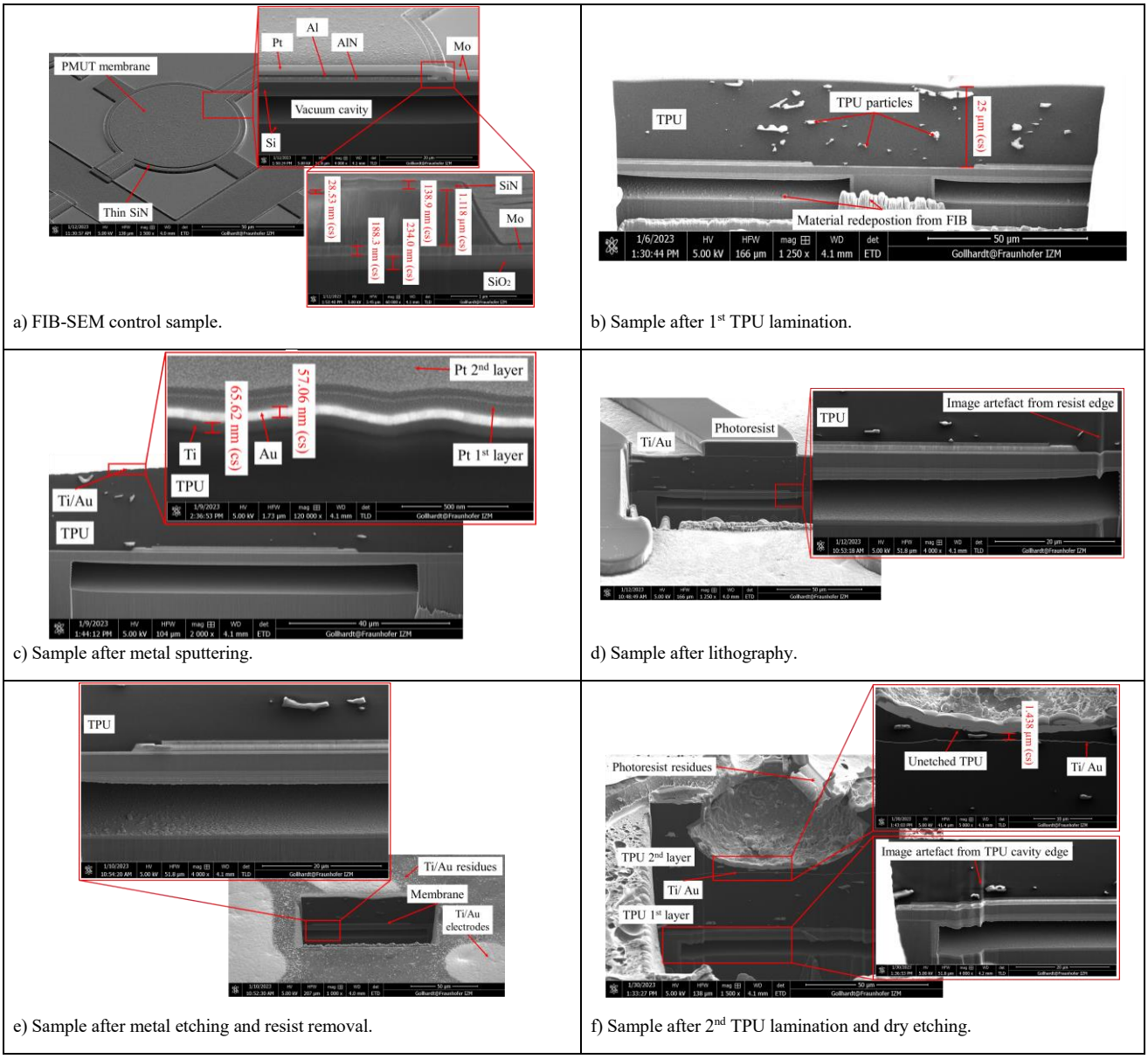

a) FIB-SEM control sample.

b) Sample after 1st TPU lamination.

c) Sample after metal sputtering.

d) Sample after lithography.

e) Sample after metal etching and resist removal.

f) Sample after 2nd TPU lamination and dry etching.

Figure 6. FIB-SEM analysis of the manufactured samples after each fabrication process step.

These are not a consequence of contamination during fabrication, as all process steps were performed in a clean environment. However, the exact nature of these particles is unknown, and the material supplier could not provide further details. Another aspect related to the creation of the FIB cuts is the material redeposition in some areas across the sample. Nevertheless, this does not have a negative impact on the overall results. **Figure 6c** shows the structure of the membranes after sputtering the stack of biocompatible metals (Ti and Au) on top of TPU. As observed, the membrane remains stable after this second step. The layer thicknesses are as expected (~50 nm of Ti and ~50 nm of Au), with a slight variation, within the accepted tolerance ranges. The two platinum (Pt) layers present above the sputtered layer are not part of the final device; however, they provide additional protection for the inspected layer during the ion beam bombardment used for the analysis. It can be noted that the surface of the TPU layer is not perfectly flat. This is because the vacuum applicator used for lamination requires the use of anti-adhesive mats on its top and bottom plates. When pressed against the sample, the non-uniformities present on the surface of these mats are also transferred to the TPU layer. **Figure 6d** illustrates the layer stack and structure of the sample after the lithography process. Despite the additional layers having different properties, thicknesses and stiffness coefficients, the membrane of the PMUT array is undamaged. **Figure 6e** shows the sample after metal etching and photoresist removal. The location of the metal electrodes and the alignment to the underlying membrane can be clearly observed. Important to note is the presence of metal residues due to the manual nature of the etching process. At this point, a short over-etching step is recommended to ensure that the sample is free of residues, which, if present in large amounts, can even lead to unwanted short circuits between the electrodes or tracks. Finally, **figure 6f** shows the complete structure of the sample, including the final TPU encapsulation and exposure of the electrodes. Since the metal layer is no thicker than 100 nm, a laser patterning technique [12], which would have reduced the number of processing steps, could not be employed. Instead, dry etching of TPU was chosen for this step. The thick photoresist layer used here as a mask was also partly consumed during the process, and as observed in **figure 6f**, some residues are present in the opened area. For this study, the aim was to investigate the effect each critical fabrication step has on the integrity of the membranes, and as shown, no negative results were recorded. Therefore, optimising the final TPU etching step will be considered in the future. This would require, first, the use of a metal hard mask instead of a photoresist layer. Having a correct choice of materials will ensure that the masking layer will not be consumed during the process, and thus, no residues should be redeposited in the opened areas. Moreover, the etching time for such diameters has to be increased to remove the final, 1 µm-thick TPU from the surface of the metal electrodes.

IV. Conclusion

This paper presents feasibility proof for the development of a miniaturized multimodal investigation tool comprising both PMUTs and MEAs. In particular, we have demonstrated that soft MEAs, can be developed, in a non-monolithic approach, on the surface of pre-existing PMUTs, without negatively affecting the integrity of the membranes throughout a variety of process steps, including, sputtering of metals, wet etching and polymer lamination under high temperature and pressure. This work could serve as a stepping stone in integrating several neuromodulation and recording modalities on the same miniaturized in-vitro investigation tool to enable a better understanding of the various neuromodulation mechanisms.

Acknowledgment

We acknowledge our colleagues Sven Schmidt and Friedrich Leonhard Schein, from the Fraunhofer Institute for Reliability and Microintegration IZM, Berlin, Germany for their support offered throughout the project.

References

[1] V. Giagka and W. A. Serdijn, "Realizing flexible bioelectronic medicines for accessing the peripheral nerves – technology considerations," *Bioelectron. Med.,* vol. 4, no. 8, pp. 1-10, June 2018, doi: https://doi.org/10.1186/s42234-018-0010-y.

[2] J. Dragas et al., "In Vitro Multi-Functional Microelectrode Array Featuring 59 760 Electrodes, 2048 Electrophysiology Channels, Stimulation, Impedance Measurement, and Neurotransmitter Detection Channels," *IEEE JSSC,* vol. 52, no. 6, pp. 1576-1590, June 2017, doi: 10.1109/JSSC.2017.2686580.

[3] A. Branner, R. B. Stein, E. Fernandez, Y. Aoyagi and R. A. Normann, "Long-term stimulation and recording with a penetrating microelectrode array in cat sciatic nerve," *IEEE TBME,* vol. 51, no. 1, pp. 146-157, January 2004, doi: 10.1109/TBME.2003.820321.

[4] M. E. Downs, S. A. Lee, G. Yang, S. Kim, Q. Wang and E. E. Konofagou, "Non-invasive peripheral nerve stimulation via focused ultrasound in vivo," *Phys. Med. Biol.,* vol. 63, no. 3, January 2018, doi: 10.1088/1361-6560/aa9fc2.

[5] V. Cotero et al., "Noninvasive sub-organ ultrasound stimulation for targeted neuromodulation," *Nat. Commun.,* vol. 10, no. 952, March 2019, doi: https://doi.org/10.1038/s41467-019-08750-9.

[6] S. Kawasaki et al., "Pressure measurement of geometrically curved ultrasound transducer array for spatially specific stimulation of the vagus nerve," in *2019 9th Int. IEEE Conf. NER*, San Francisco, CA, USA, 2019, doi: 10.1109/NER.2019.8717064.

[7] T. Costa, C. Shi, K. Tien, J. Elloian, F. A. Cardoso and K. L. Shepard, "An Integrated 2D Ultrasound Phased Array Transmitter in CMOS With Pixel Pitch-Matched Beamforming," *IEEE TBioCAS,* vol. 15, no. 4, pp. 731-742, August 2021, doi: 10.1109/TBCAS.2021.3096722.

[8] Position II Consortium, "White paper discussing different technology variants in relation to the application matrix," ECSEL 2017-3-783132 POSITION II project.

[9] K. Nanbakhsh, R. Ritasalo, W. A. Serdijn and V. Giagka, "Long-term Encapsulation of Platinum Metallization Using a HfO2 ALD - PDMS Bilayer for Non-hermetic Active Implants," in *2020 70th Int. IEEE Conf. ECTC*, Orlando, FL, USA, 2020, doi: 10.1109/ECTC32862.2020.00081.

[10] Y. S. Choi et al., "Stretchable, dynamic covalent polymers for soft, long-lived bioresorbable electronic stimulators designed to facilitate neuromuscular regeneration," *Nat. Commun.,* vol. 11, no. 5990, November 2020, doi: https://doi.org/10.1038/s41467-020-19660-6.

[11] A. Pak et al., "Thermoplastic polyurethane as a base material for flexible neural interfaces," *in preparation.*

[12] A. I. Velea et al., "UV and IR Laser-Patterning for High-Density Thin-Film Neural Interfaces," in *2021 23rd Int. IEEE Conf. EMPC*, Gothenburg, Sweden, 2021, doi: 10.23919/EMPC53418.2021.9584962.